CrystEngComm

Accepted Manuscript

ROYAL SOCIETY OF CHEMISTRY

www.rsc.org/crystengcomm

Journal Name

RSCPublishing

ARTICLE

Acid-induced Zn(II)-based metal-organic framework for encapsulation and sensitization of lanthanide cations

Cite this: DOI: 10.1039/xoxxooooox

Hongjie He,[a] Lina Zhang[b], Mingli Deng,[a] Zhenxia Chen,*[a] Yun Ling,[a] Jinxi Chen,*[b] Yaming Zhou[a]

Received ooth January 2012,
Accepted ooth January 2012

DOI: 10.1039/xoxxooooox

www.rsc.org/

Two Zn(II)-based metal-organic frameworks, namely, $[Zn_3(Hbptc)_2(DMF)_2]\cdot 2DMF$(**1**) and $[Zn_5(bptc)_3(H_2O)](((CH_3)_2NH_2)_2$(**2**), ($H_4$bptc = 3,3',5,5'-biphenyltetracarboxylic acid, DMF = N,N'-dimethylformamide), have been synthesized using different amounts of nitric acids under the mixed-solvothermal condition. **1** and **2** display different coordination geometries and donor ligands for the Zn^{2+} ions. In **1**, only three carboxylic acid groups of H_4bptc take part in the construction of the three-dimensional (3-D) framework with Zn^{2+}, and one remains uncoordinated that can bind to other metal ions. Postsynthetic exchange of **1** with Ln^{3+} cations demonstrate that **1** can effectively capture metal cations and sensitize the visible-emitting Ln^{3+}.

Introduction

Metal-organic frameworks (MOFs) assembled from metal-based nodes and organic linkers are a promising new class of materials,[1] which have been widely studied on account of their possible applications in the fields including catalysis,[2] gas separation,[3] gas storage,[4] molecular recognition,[5] drug delivery,[6] and magnetism,[7] etc. The rational design and syntheses are of vital importance to get MOFs with special properties. In the aspect of design, the organic ligands with desired functional groups such as -OH[8], -NH_2[9] and -NO_2[10] are often chosen. However, controllable synthesis of these predicted compounds is still a great challenge because the formation of target MOFs is highly influenced by a variety of factors, such as solvent,[11] pH value of the solution,[12] reaction time,[13] and temperature,[14] etc. To remain at least one carboxylate group uncoordinated as a functional site, the selection of polycarboxylate ligands is one key factor in the assembly process of the desired MOFs. In this work, we used a rigid tetracarboxylate ligand of 3,3',5,5'-biphenyltetracarboxylic acid (H_4bptc), which owns four carboxylic acids allowing for partial or total deprotonation, involving rich coordination modes to form various structures.[13,15,16]

When controllable synthesis is used as a method to introduce uncoordinated carboxyl groups into MOFs, they would be versatile and accessible materials via a post-synthetic modification (PSM) strategy.[17] PSM is employed as an effective tool to imbue MOFs with enhanced performance characteristics.[18] For example, Lanthanide ions can be introduced into MOFs undergoes postsynthetic modification by means of ion exchange.[19] The unique optical properties of Ln doped MOFs make them especially attractive for potential applications in fluorescence probes.[20] MOF can serve as both a host and an antenna for protecting and sensitizing extra-framework lanthanide cations. Herein, we reported two Zn-based MOFs, namely, $[Zn_3(Hbptc)_2(DMF)_2]\cdot 2DMF$ (**1**) and $[Zn_5(bptc)_3(H_2O)]\cdot 2(CH_3)_2NH_2$ (**2**) by controlling the amount of nitric acids in the reaction. Compound **1** remains uncoordinated carboxyl groups pointing to the interior of pores, which provide as PSM sites to capture Ln^{3+} ions. **1** effectively serve as an antenna for sensitizing the visible-emitting Ln^{3+} cations.

Experimental section

Materials and general measurements

The H_4bptc ligand was synthesized using procedures reported previously.[15c] Other materials were reagent grade obtained from commercial sources and used as received. Powder X-ray diffraction (PXRD) patterns were measured using a Bruker D8 powder diffractometer at 40 kV, 40 mA with Cu Kα radiation (λ = 1.5406 Å), with a scan speed of 0.2 s/step and a step size of 0.02° in the 2θ region 5-50°. Thermogravimetric analyses (TGA) were carried out with a METTLER TOLEPO TGA/SDTA851 analyzer in the temperature range of 30-800 °C under N_2 flow with a heating rate of 10 °C·min^{-1}. Elemental analysis for C, H, N were done on the Elementar Vario EL III microanalyzer. IR spectra were measured on KBr pellets on a Nicolet Nexus 470 FT-IR spectrometer in the range of 4000-400 cm^{-1}. Photoluminescence measurements were performed on a Hitachi F-4500 fluorescence spectrophotometer equipped with monochromator (resolution = 0.2 nm) and a 150W Xe lamp at room temperature in solid states. A Micromeritics ASAP 2020 surface area analyzer was used to measure gas adsorption. Before the measurement, about 100 mg

of as-made samples were exchanged with acetone for three days and activated at 140 °C for 5 hours by using the "outgas" function of the analyzer.

Synthesis of $[Zn_3(Hbptc)_2(DMF)_2]\cdot 2DMF$ (1). $Zn(OAc)_2\cdot 2H_2O$ (0.15mmol, 0.034 g) and H_4bptc (0.10mmol, 0.033g) were dissolved in mixed solvents of N,N'-dimethylformamide (DMF) (2.0 mL) and isopropanol (IPA) (0.5 mL). Twelve drops of 68 wt% nitric acid (about 0.6 mL) were added and the mixture was further stirred for 30 min. The resulted white gel was sealed in a Telflon-lined stainless steel autoclave (15 mL) and heated at 140 °C for 3 days, followed by slow cooling down to room temperature. Yellowish rod-like crystal products were collected by filtration and then washed with 5mL DMF (yield: 46% for **1** based on H_4bptc). Elemental analysis calcd for 1($C_{44}H_{42}N_4O_{20}Zn_3$): C 46.20, H 3.67, N 4.90%; found: C 46.26, H 3.64, N 4.86%. IR (KBr pellets, cm^{-1}):3432(br), 3074(w), 2917(w), 1704(w), 1656(s), 1562(m), 1490(w), 1432(m), 1376(s), 1230(w), 1099(w), 905(w), 763(m), 725(m), 651(m).

Synthesis of $[Zn_5(bptc)_3(H_2O)]\cdot 2(CH_3)_2NH_2$ (2). 2 was synthesized by a similar reaction to that for **1**, except that the amount of 68 wt% nitric acid was eight drops (about 0.4 mL). Colorless block crystal products were collected by filtration (yield: 51% for **2** based on H_4bptc). Elemental analysis calcd for 2 ($C_{52}H_{36}N_2O_{25}Zn_5$): C 44.08, H 2.54, N 1.98%; found: C 44.12, H 2.57, N 1.96%. IR (KBr pellets, cm^{-1}): 3442(br), 2931(w), 1629(s), 1577(s), 1405(m), 1365(s), 1249(w), 1085(w), 1020(w), 914(w), 823(w), 771(m), 729(m), 659(m).

Preparation of Na@1, Cu@1 and Ln@1 (Ln = Sm, Eu, Dy and Tb).

Saturated solution of $NaHCO_3$ in acetone and Ln^{3+} nitrate in acetone (0.01 M) were prepared in advance. **1** was exchanged with acetone for three days and heated at 140 °C under vacuum to give **1a**.

Na@**1**: **1a** (~100 mg) was soaked with $NaHCO_3$ solution (10mL), slowly volatilized acetone and replenished new solution every day. After two weeks, the material was washed with acetone for five times and thereafter soaked in acetone (at least two days).

Cu@**1**: A few activated samples of **1a** were directly immersed in acetone solution of copper nitrate, and slowly volatilized acetone. After one week, a sample of Cu@**1** was washed with acetone and thereafter soaked in acetone (at least two days).

Ln@**1**: Na@**1** (~80 mg) was soaked in Ln^{3+} nitrate solution (10mL), slowly volatilized acetone and replenished new solution. After repeated this procedure for two weeks, the materials were thoroughly washed with acetone and thereafter soaked in acetone (at least two days).

Crystal data collection and refinement

Data collection for **1** and **2** was carried out on a Bruker Apex CCD diffractometer with graphite monochromated Mo Kα radiation (λ = 0.71073 Å) at 293 K. Data reduction was performed with SAINT, and empirical absorption corrections were applied by the SADABS program[21]. Structures were solved by direct methods using the SHELXS program and refined with the SHELXL program.[22] Heavy atoms and other non-hydrogen atoms were directly obtained from a difference Fourier map. Final refinements were performed by full-matrix least-squares methods with anisotropic thermal parameters for all non-hydrogen atoms on F^2. C-bonded H atoms were placed geometrically and refined as riding modes. The molecular formulae are determined according the single crystal X-ray diffraction data. Crystallographic data are listed in Table 1, and selected bond length and angles are listed in Table S1†.

Table 1 Crystal and structure refinement data for **1** and **2**

	1	**2**
Empirical formula	$C_{44}H_{42}N_4O_{20}Zn_3$	$C_{52}H_{36}N_2O_{25}Zn_5$
Formula weight	1142.92	1415.68
Temperature (K)	293(2)	293(2)
Wavelength (Å)	0.71073	0.71073
Crystal system	Monoclinic	Monoclinic
Space group	*C* 2/c	*C* 2/c
a (Å)	16.646(6)	12.145(11)
b(Å)	18.345(7)	30.72(3)
c(Å)	16.309(6)	22.75(2)
β (°)	108.893(4)	94.000(12)
V (Å^3)	4712(3)	8468(13)
Z	4	4
D_c *(g cm^{-3})*	1.611	1.110
μ(mm^{-1})	1.599	1.454
F(000)	2336	2848
Total collected	7790	20605
Unique data, R_{int}	3797, 0.0540	7520, 0.0728
GOF on F^2	0.954	0.934
R_1[a],wR_2[b] [I>2σ(I)]	0.0473, 0.1199	0.0619, 0.1885
R_1, wR_2(all data)	0.0687, 0.1342	0.0792, 0.2021
$\Delta\rho_{max}/\Delta\rho_{min}$ (e·Å^{-3})	0.885, -0.636	1.229, -1.071

[a] $R_1 = \Sigma||F_o| - |F_c||/\Sigma|F_o|$. [b] $wR_2 = [\Sigma w(F_o^2 - F_c^2)^2/\Sigma w(F_o^2)^2]^{1/2}$

Results and discussion

Synthesis

1 was obtained by the solvothermal reaction of H_4bptc with $Zn(OAc)_2\cdot 2H_2O$ in the mixed solution of DMF and isopropyl alcohol with the addition of twelve drops of 68 wt% nitric acids. Under this condition, one carboxyl group of H_4bptc in **1** remains uncoordinated according to the single X-ray structure. The synthesis procedure of **2** was similar to that of **1**, except that eight drops of nitric acids were used. In this condition, all the carboxylate groups were involved in metal coordination. In the procedure of synthesis, the amount of acids would greatly affect the generated products. To confirm this, all other things being equal, different amount of nitric acids were introduced to the reaction system. When more than fifteen drops of acids (~0.75 mL) were added, only clear liquor was obtained. Reaction without any acids results in white powders identified as an unknown phase. Other acids, including H_2SO_4 and HCl were also used under the condition of reaction **1**. PXRD

patterns of the products do not match either **1** or **2** (Fig. S1†), indicating HNO_3 plays important role in the formation of both structures.

Structural description

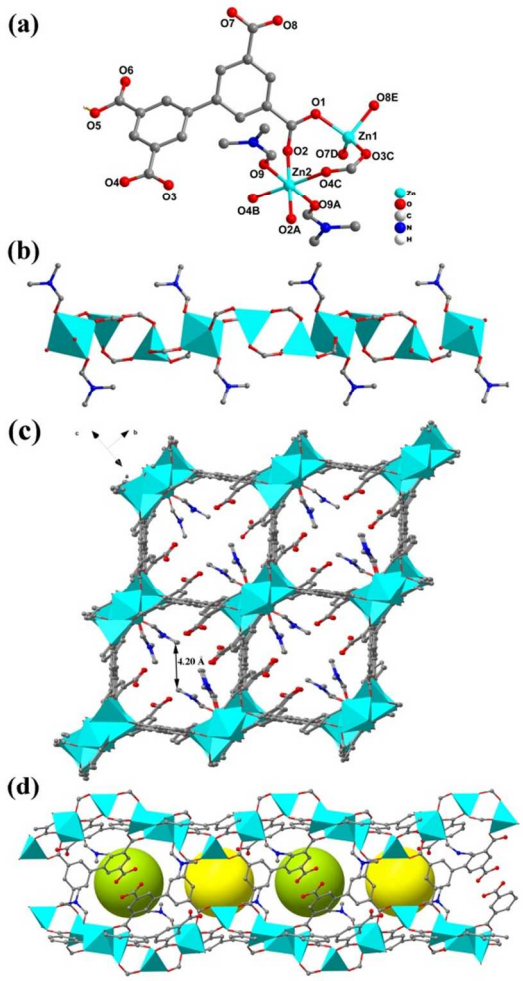

Fig. 1: (a) The coordination environment of Zn in **1** (symmetry code used: A: 0.5-x,0.5-y,1-z; B: 1-x,y,1.5-z; C: -0.5+x, 0.5-y,-0.5+z; D: x,-y,-0.5+z; E:-x, -y,1-z). (b)The chain consists of ZnO_4, ZnO_6 and carboxylate. (c) 3-D structure showing 1-D channels (the guest DMF are omitted for clarity). (d) Schematic representation of two kinds of cage-like spaces inside one channel.

Crystal structure of 1. Single crystal X-ray diffraction analysis reveals that **1** crystallizes in the monoclinic space group *C*2/c. **1** contains one independent zinc atom (Zn1) and another another zinc (Zn2) with half occupation lies on an inversion centre. The ligand is partial deprotonated as $Hbptc^{3-}$ and one coordinated and another guest DMF molecules are located in the asymmetric unit. As depicted in Fig. 1a, the Zn ions have two modes of coordination, Zn1 is four-coordinated by four oxygen atoms from different $Hbptc^{3-}$ ligands [Zn-O = 1.932(3), 1.940(3), 1.948(3) and 1.973(3) Å] to finish a [ZnO_4] tetrahedron geometry; the Zn2 ion is linked by six oxygen atoms from four different $Hbptc^{3-}$ ligands [Zn-O =2.041(3) and 2.078(3)Å] and two symmetrical DMF molecules [Zn-O = 2.090(4)Å], resulting in a [ZnO_6] octahedron geometry. Three carboxylate groups on the $Hbptc^{3-}$ ligand have close C-O bond distances ranging from 1.222(6) to 1.277(5) Å. However, the fourth uncoordinated carboxyl group has two distinguishable C-O bond distances of 1.314(7) and 1.220(7) Å. O5 with the longest C-O bond was then designated as a hydroxyl group. The units of [ZnO_4] and [ZnO_6] are linked together via carboxylate groups to form an infinite chain (Fig. 1b). The neighbouring chains are further linked by $Hbptc^{3-}$ ligands, resulting in a three-dimensional (3-D) framework with 1-D channels (Fig. 1c). The coordinated DMF molecules and uncoordinated carboxyl groups protrude into the channels and the nearest distance between the carbon atoms of DMF is 4.20 Å. Despite of the small size of the straight channel, there are two kinds of cage-like spaces with same radius of about 3.4 Å where the guest molecules of DMF reside (Fig. 1d). The accessible volume and porosity are 1134.7 $Å^3$ and 24.1%, respectively through the analysis of PLATON software.[23]

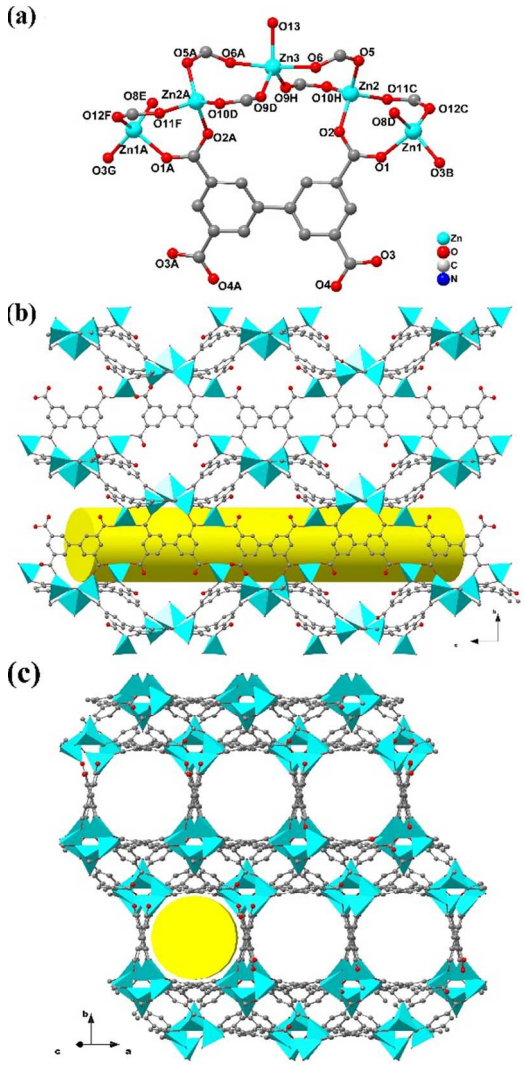

Fig. 2 (a) The coordination environment of Zn in **2** (symmetry code used: A: -x, y, 0.5-z; B: -x+0.5,-y+0.5,-z+1; C: -x+1,-y,-z+1; D: -x,-y,-z+1; E: x,-y,z+0.5; F: -1+x, -y, -0.5+z; G: -0.5+x, 0.5-y, -0.5+z; H: x, -y, z-0.5); (b) and (c) The 3-D structure constructed by wavy layers and $bptc^{4-}$ ligands, showing the 1-D straight channels (dma molecules are omitted for clarity).

Crystal structure of 2. **2** crystallized in the monoclinic space group C2/c. The asymmetric unit of **2** consists of two and a half crystallographically independent Zn^{2+} ions, of which Zn3 lies on a twofold axis with a site occupation of 0.5. There are one and a half of bptc4- ligands and the half lies about the same twofold axis. The water molecule coordinated to Zn3 is located on the same axis and the guest dimethylammonium (dma) cation is assigned as protonated to keep charge balance. As shown in Fig. 2a, both Zn1 and Zn2 centers coordinated with four oxygen atoms from different $bptc^{4-}$ ligands in a tetrahedral fashion. The average bond distances of Zn1–O and Zn2–O are 1.94 Å and 1.93 Å, respectively. Zn3 center is linked by five oxygen atoms from four different $bptc^{4-}$ ligands [Zn–O =2.136(5) and 1.978(6) Å] and one coordinated H_2O molecule [Zn–O = 1.995(14) Å], forming a triangle bipyramid [ZnO_5] coordination geometry. The units of four [ZnO_4] and one [ZnO_5] are connected together via carboxylate groups to construct a subunit of [$Zn_5O_5(CO_2)_8$]. Those subunits are linked together by one $bptc^{4-}$ ligand to form a wavy layer, which are then connected by the other $bptc^{4-}$ ligand into a 3-D framework (Fig. 2b). The resulting structure contains 1-D cylindrical channels with the radius of about 4.5 Å (Fig. 2c). Calculations using PLATON showed that the effective volume is 3858.9 $Å^3$ per unit cell after removing the guest molecules, which is 45.6% void space to the total crystal volume.

PXRD and TG measurements

The experimental and simulated powder X-ray diffraction (PXRD) patterns of compounds **1** and **2** confirmed the purities of the synthesized crystalline samples (Fig. S1†). Thermogravimetric analysis (TGA) was conducted to investigate the thermal stability of compounds **1** and **2** (Fig. S2†). As observed from the TGA curve of **1**, there is loss of two guest DMF molecules (found 13.07%, calcd. 12.95%) from 127 to 218°C, then its coordinated DMF molecules start to decompose thermally to 380 °C (found 12.62%). After that, the organic components start to decompose. TGA data of **2** reveals a continuous weight loss of about 32.49% from 30 to about 250°C, which is higher than that of dma molecules in the formula. This might be ascribed to the presence of physically adsorbed water molecules. Further increasing the temperature will lead to the loss of organic ligands, accompanying the decomposition of the framework.

Gas adsorption

Samples **1** and **2** were exchanged with acetone for 3 days, totally 9 times and then heated at 140°C under vacuum before the adsorption. Due to the TGA and varied-temperature PXRD analyses, the guest molecules of DMF and protonated $Hdma^+$ molecules in **1** and **2** could not be totally removed without losing the structural integrities. So there is no significant adsorption of N_2 at 77K. However, as shown in Fig. 3, **1** and **2** did have moderate adsorption capacities for CO_2 adsorption. Both of them show type-I adsorption isotherms. The adsorption amount of activated **1** at 1.05 bar is 1.53mmol·g^{-1} at 273 K and 0.84mmol·g^{-1} at 298 K, and for activated **2** is 1.34mmol·g^{-1} and 0.49mmol·g^{-1} respectively. The CO_2 adsorption capacity of **1** is higher than **2** despite the lower calculated pore volume. Such a particular result may be related to the weak interaction of CO_2 with uncoordinated carboxyl groups in the pores of **1**. The integrity of the frameworks after sorption was confirmed by PXRD patterns (Fig. S1b†).

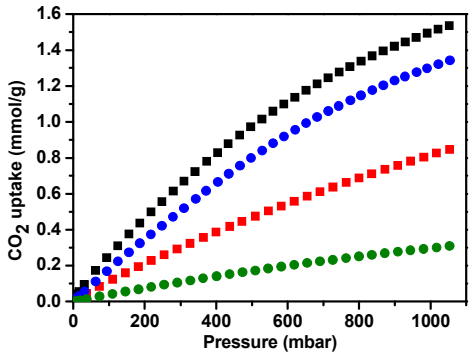

Fig. 3: CO_2 sorption isotherms for **1** (black squares: at 273 K, red squares: at 298 K) and **2** (blue circles: at 273K, green circles: at 298K)

Capture of metal cations

Compound **1** with uncoordinated free carboxyl groups binding sites inspires us to incorporate sodium cations in a postsynthetic fashion. Liu et. al have reported that the carboxyl group can be deprotonated by MeONa via a straightforward acid-base reaction.[17a] Herein, Na@**1** was prepared in a milder way by soaking activated compound **1** in the saturated solution of $NaHCO_3$ solution of acetone for two weeks. Then the metal ions could easily take up the exchanged position into the pores replacing Na^+. Cu^{2+} was chosen to monitor the exchange processes, for its special colour can be distinguished by the naked eye (Fig. S3†). The obtained sample of Cu@**1** with a bluish tint visually means Ln@**1** can be accomplished by soaking Na@**1** in lanthanide metal ion solution for enough time. As expected, similar experiment results were achieved when use Ln^{3+} nitrate solution. In this way, metal-cations-captured compounds Ln@**1** (Ln = Sm, Dy, Eu and Tb) were formed without destroying the original crystalline integrity, as confirmed by the powder X-ray diffraction patterns (Fig. S4†).

The solid-state photoluminescent properties of each sample were investigated at room temperature (Fig. S5†). The free H_4bptc ligand displayed one emission peak at 370 nm under excitation at 316 nm, which might come from the π–π* interactions between the aromatic rings of the ligand. The emission peak of compound **1** at about 460 nm was measured with the excitation wavelength of 385 nm, which may be ascribe to the ligand-to-metal charge transfer (LMCT), that could be observed in many zinc-carboxylate systems.[24] Using the similar excitation, Na@**1** displayed broad-band blue emission in the range of 400-500 nm.

In further experiments, all the Ln@**1** samples after postsynthetic modification have their own characteristic emission

peaks, in addition to the emission range of 400-500 nm corresponding to the framework emission (Fig. 4). When excited at wavelength of 325 nm, Sm@**1** showed very weak emission peaks [562 nm ($^4G_{5/2}$ →$^6H_{5/2}$), 597 nm ($^4G_{5/2}$→$^6H_{7/2}$)]. Dy@**1** displayed very similar emission to Sm@**1** with two weak characteristic emissions [542nm ($^4F_{9/2}$→$^6H_{13/2}$), 573nm ($^4F_{9/2}$→$^6H_{11/2}$)]. Eu@**1** had three characteristic emission peaks [592 nm ($^5D_0$→$^7F_1$), 614 nm ($^5D_0$→$^7F_2$), and 696 nm ($^5D_0$→$^7F_4$)]. When excited with a UV lamp (254nm), this sample emitted a distinguishable dark-red colour. Interesting result was given by comparative analysis of the Tb@**1**, significant lanthanide-centered emissions of Tb^{3+} [490 nm ($^5D_4$→$^7F_6$), 544 nm ($^5D_4$→$^7F_5$)] were detected when excited at 303 nm wavelength, and the emission corresponding to the frameworks was suppressed by the energy transfer and nearly disappeared. Impressively, bright green colour could be observed by naked eye under a UV lamp excited at 254 nm as a distinctive indication of Tb^{3+} sensitization.

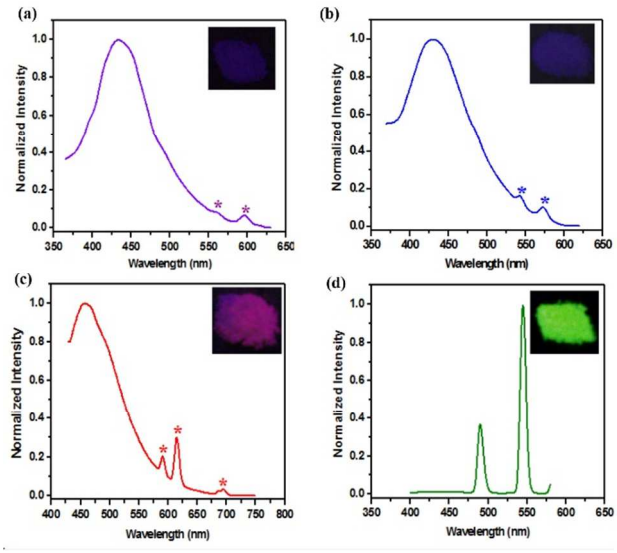

Fig. 4: Photoluminescence spectra of Ln@**1**, inset shows the corresponding sample under a 254 nm laboratory UV light. (a): Sm@**1**; (b): Dy@**1**; (c): Eu@**1**; d: Tb@**1**.

As we know, lanthanide cations-centered emission spectra are assigned to 4f→4f or 4f→4d transitions, generally for the former. The transitions are forbidden under free state, nonetheless, it can be sensitized by electron conjugated systems with efficient energy-transfer, which was called "antenna effect".[25] It is obvious that the ordered MOF **1** became a sensitizer for the lanthanide-centered emission. The excitation light was absorbed by the biphenyl moiety in the structure and subsequently efficiently transferred to the lanthanide ions through the MOF structure, which can exhibit enhanced characteristic fluorescence signal (Fig. 5). On account of the different energy gap of various lanthanide ions, MOF **1** cannot efficiently sensitize the Sm^{3+}, Dy^{3+}, Eu^{3+} luminescence, resulting in different intensity emissions. Tb@**1** exhibited a strong luminescence emission in this case, demonstrated that MOF **1** is suitable for the sensitization of Tb^{3+} ion rather than Sm^{3+}, Dy^{3+} and Eu^{3+} emitter. The selectivity is different from other reported MOFs.[19]

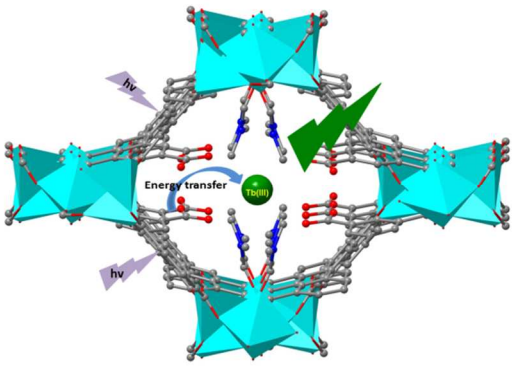

Fig. 5: Schematic illustration of the generation mechanism of green emission of Tb^{3+}@**1**

Conclusions

In this paper, two three-dimensional porous MOF structures $[Zn_3(Hbptc)_2(DMF)_2]\cdot 2DMF$(**1**) and $[Zn_5(bptc)_3(H_2O)]((CH_3)_2NH_2)_2$(**2**) have been successfully synthesized under solvothermal conditions via regulation of the amount of nitric acids. Compound **1** features uncoordinated carbonyl groups stretching into the pores, which act as functionalization sites for capturing lanthanide ions and demonstrated luminescent sensitization for Ln^{3+} ion via post-synthetic modification. This study demonstrates that the coordination geometries of a polycarboxylic acid can be adjusted by the synthetic process to form MOFs with uncoordinated carboxyl groups. It is clear that the availability of free carboxyl sites may confer unique functionality on this class of materials, for further exploring and expanding their properties, as demonstrated hereby the capture of cations with fluorescence.

Acknowledgements

This work was financially supported by NSFC (Nos. 21101031, 21203032, and 21171042), the Program for Changjiang Scholars and Innovative Research Team in University (IRT1117) and Shanghai Leading Academic Discipline Project (Project No. B108).

Notes and references

[a] Department of Chemistry, Fudan University, Shanghai 200433, P. R. China. E-mail: zhxchen@fudan.edu.cn
[b] School of Chemistry and Chemical Engineering, Southeast University, Nanjing 211189, P. R. China. E-mail: chenjinxi@seu.edu.cn

Electronic Supplementary Information (ESI) available: Details of TG results and PXRD patterns. CCDC 1032538 (**1**) and 1032539 (**2**) contains the supplementary crystallographic data for this paper. For ESI and crystallographic data in CIF or other electronic format, see DOI: 10.1039/b000000x/

1 (a) S. Kitagawa, R. Kitaura and S. Noro, *Angew. Chem. Int. Ed.*, 2004, **43**, 2334-2375; (b) J. L. C. Rosell and O. M. Yaghi, *MicroporousMesoporous Mater.*, 2004, **73**, 3-14; (c) M. Eddaoudi, D. B. Moler, H. L. Li, B. L. Chen, T. M. Reineke, M. O'Keeffe and

O. M. Yaghi, *Acc. Chem. Res.*, 2001, **34**, 319-330; (d) B. Moulton and M. J. Zaworotko, *Chem. Rev.*, 2001, **101**, 1629-1658.

2 (a) M. Yoon, R. Srirambalaji and K. Kim, *Chem. Rev.*, 2012, **112**, 1196-1231; (b) M. H. Xie, X. L. Yang and C. D. Wu, *Chem. Commun*., 2011, **47**, 5521-5523; (c) D. Liu, Z. G.Ren, H. X. Li, J. P. Lang, N. Y. Li and B. F. Abrahams, *Angew. Chem. Int. Ed.,* 2010, **49**, 4767-4770; (d) J. Lee, O. K. Farha, J. Roberts, K. A. Scheidt, S. T. Nguyenand J. T. Hupp, *Chem. Soc. Rev*., 2009, **38**, 1450-1459.

3 (a) Q. Y. Yang, D. H. Liu, C. L. Zhong and J. R. Li, *Chem. Rev.,* 2013, **113**, 8261-8323; (b) J. R. Li, R. J. Kuppler and H. C. Zhou, *Chem. Soc. Rev*., 2009, **38**, 1477-1504.

4 (a) S. Q. Ma and H. C. Zhou, *Chem. Commun*., 2010, **46**, 44-53; (b) L. J. Murray, M. Dincă and J. R. Long, *Chem. Soc. Rev*., 2009, **38**, 1294-1314.

5 (a) Y. Li, S. S. Zhang and D. Song, *Angew. Chem. Int. Ed.*, 2013, **52,** 710-713; (b) Z. G. Xie, L. Q. Ma, K. E. deKrafft, A. Jin and W. B. Lin, *J. Am. Chem. Soc*., 2010, **132**, 922-923; (c) G. Lu and J. T. Hupp, *J. Am. Chem. Soc.*, 2010, **132**, 7832-7833.

6 (a) D. Cunha, M. B. Yahia, S. Hall, S. R. Miller, H. Chevreau, E. Elkaïm, G. Maurin, P. Horcajada and C. Serre, *Chem. Mater*., 2013, **25**, 2767-2776; (b) J. D. Rocca, D. M. Liu and W. B. Lin, *Acc. Chem. Res.,* 2011, **44**, 957-968; (c) F. Ke, Y. P. Yuan, L. G. Qiu, Y. H. Shen, A. J. Xie, J. F. Zhu, X. Y. Tian and L. D. Zhang, J. *Mater. Chem.*, 2011, **21**, 3843-3848.

7 (a) M. Wriedt, A. A. Yakovenko, G. J. Halder, A. V. Prosvirin, K. R. Dunbar and H. C. Zhou, *J. Am. Chem. Soc*., 2013, **135,** 4040-4050; (b) W. Zhang and R.G. Xiong, *Chem. Rev.,* 2012, **112**, 1163-1195; (c) P. Dechambenoitand J. R. Long, *Chem. Soc. Rev.*, 2011, **40**, 3249-3265.

8 Z. X. Chen, S. C. Xiang, H. D. Arman, P. Li, S. Tidrow, D.Y. Zhao and B. L. Chen, *Eur. J. Inorg. Chem*., 2010, 3745-3749.

9 A. Shigematsu, T. Yamada and H. Kitagawa, *J. Am. Chem. Soc*., 2011, **133**, 2034-2036.

10 K. Uemura, Y. Yamasaki, F. Onishi, H. Kita and M. Ebihara, *Inorg. Chem.,* 2010, **49**, 10133-10143.

11 (a) M. Mazaj, T. B. Čelič, G. Mali, M. Rangus, V. Kaučič and N. Z. Logar, *Cryst. Growth Des.*, 2013, **13**, 3825-3834; (b) F. Y. Yi and Z. M. Sun, *Cryst. Growth Des.*, 2012, **12**, 5693-5700; (c) Y. Q. Lan, H. L. Jiang, S. L. Li and Q. Xu, *Inorg. Chem*., 2012, **51**, 7484-7491.

12 P. D. C. Dietzel, R. Blom and H. Fjellvåg, *Eur. J. Inorg. Chem.,* 2008, 3624-3632.

13 B. L. Chen, N. W. Ockwig, F. R. Fronczek, D. S. Contreras and O. M. Yaghi, *Inorg. Chem.*, 2005, **44**, 181-183.

14 (a) S. S. Nagarkar, A. K. Chaudhari and S. K. Ghosh, *Cryst. Growth Des*., 2012, **12**, 572-576; (b) J. J. Wu, W. Xue, M. L. Cao, Z. P. Qiao and B. H. Ye, *CrystEngComm*, 2011, **13**, 5495-5501; (c) J. J. Zhang, L.Wojtas, R. W. Larsen, M. Eddaoudi and M. J. Zaworotko, *J. Am. Chem. Soc.,* 2009, **131**, 17040-17041.

15 (a) Q. P. Lin, T. Wu, S. T. Zheng, X. H. Bu, P. Y. Feng, Chem. Commun., 2011, **47**, 11852-11854; (b) J. J. Wang, P. X. Cao, L. J. Gao, F. Fu, M. L. Zhang, Y. X. Ren, X. Y. Hou, *Chinese J. Struct. Chem.*, 2011, **30**, 1787-1790; (c) F. L. Yang, Q. S. Zheng, Z. X. Chen, Y. Ling, X. F. Liu, L. H. Weng and Y. M. Zhou, *CrystEngComm*, 2013, **15**, 7031-7037; (d) X. T. Zhang, L. M. Fan, Z. Sun, W. Zhang, D. C. Li, J. M. Dou, L. Han, *Cryst. Growth Des.*, 2013, **13**, 792-803; (e) Q. P. Li, J. J. Qian, *RSC Adv.*, 2014, **4**, 32391-32397; (f) W. J. Zhao, J. T. Tan, X. Li, Y. L. Lu, X. Feng, X. W. Yang, *Chem. Pap*., 2014, **68**, 1415-1420.

16 B. L. Chen, N. W. Ockwig, A. R. Millard, D. S. Contreras, O. M. Yaghi, *Angew Chem Int Ed*., 2005, **44**, 4745-4749.

17 (a) J. W. Cao, Y. F. Gao, Y. Q. Wang, C. F. Du and Z. L. Liu, *Chem. Commun.,* 2013, **49**, 6897-6899; (b) Y. Zhou and B. Yan, *Inorg. Chem*., 2014, **53**, 3456-3463. (c) Y. Zhou, H. H. Chen, B. Yan, *J. Mater. Chem. A*, 2014, **2**, 13691-13697; (d) J. N. Hao, B. Yan, *J. Mater. Chem. A*, 2014, **2**, 18018-18025.

18 (a) S. M. Cohen, *Chem. Rev*., 2012, **112**, 970-1000; (b) W. M. Bloch, A. Burgun, C. J. Coghlan, R. Lee, M. L. Coote, C. J. Doonan and C. J. Sumby, *Nat. Chem.*, 2014, **6** ,906-912.

19 (a) J. An, C. M. Shade, D. A. Chengelis-Czegan, S. Petoud and N. L. Rosi, *J. Am. Chem. Soc.,* 2011, **133**, 1220-1223; (b) M. L. Ma, J. H. Qin, C. Ji, H. Xu, R. Wang, B. J. Li, S. Q. Zang, H. W. Hou and S. R. Batten, *J. Mater. Chem. C.,* 2014, **2**, 1085-1093; (c) Y. Y. Liu, R. Decadt, T. Bogaerts, K. Hemelsoet, A. M. Kaczmarek, D. Poelman, M. Waroquier, V. V. Speybroeck, R. V. Deun, and P. V. D. Voort, *J. Phys. Chem. C*. 2013, **117**, 11302-11310; (d) J. S. Qin, S. R. Zhang, D. Y. Du, P. Shen, S. J. Bao, Y. Q. Lan, Z. M. Su, *Chem. Eur. J.*, 2014, **20**, 5625-5630.

20 (a) B. L. Chen, L.B. Wang, F. Zapata, G. D. Qian, and E. B. Lobkovsky, *J. Am. Chem. Soc.* 2008, **130**, 6718-6719. (b) Y. J. Cui, Y. F. Yue, G. D. Qian, B. L. Chen, *Chem. Rev.*, 2012, **112**, 1126-1162; (c) Z. C. Hu, B. J. Deibert and J. Li, *Chem. Soc. Rev.*, 2014, **43**, 5815-5840.

21 Bruker, Analytical X-ray System. SAINT+ programs, Release Version6.02, 1999.

22 (a) G. M. Sheldrick, SHELXL-2013, Program Crystal Structure Refinement, University of Göttingen, Germany, 2013; (b) G. M. Sheldrick, SHELXS-2013, Programs for X-ray Crystal Structure Solution, University of Göttingen, Germany, 2013.

23 A. L. Spek, PLATON99, A Multipurpose Crystallographic Tool, Utrecht University, Utrecht (The Netherlands), 1999.

24 (a) E. C. Yang, H. K. Zhao, B. Ding, X. G. Wang and X. J. Zhao, *Cryst. Growth Des*., 2007, **7**, 2009–2015; (b) M. Du, X. J. Jiang and X. J. Zhao, *Inorg. Chem*., 2007, **46**, 3984-3995; (c) S. L. Zheng, J. H. Yang, X. L. Yu, X. M. Chen and W. T. Wong, *Inorg. Chem.*, 2004, **43**, 830-838.

25 (a) R. Decadt, K. V. Hecke, D. Depla, K. Leus, D. Weinberger, I. V. Driessche, P. V. D. Voortand R. V. Deun, *Inorg. Chem*., 2012, **51**, 11623-11634; (b) G. Blasse and B. C. Grabmaier, *Luminescent Materials*, Springer, Berlin, 1994.

Graphical abstract

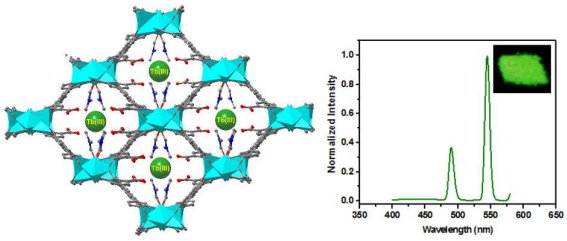

Two Zn(II)-based metal-organic frameworks with different coordination geometries have been synthesized and one can effectively capture metal cations and sensitize the visible-emitting Tb^{3+}.